Wave-Body Interaction with Overlapping Structured Grids in the HPC Method

Finn-Christian W. Hanssen*[1], Marilena Greco[1,2], Odd M. Faltinsen[1]

[1]AMOS, Marine Technology Department, NTNU, Trondheim, Norway
[2]CNR-INSEAN, Marine Technology Institute, Roma, Italy
* finn-christian.hanssen@ntnu.no

HIGHLIGHTS

A numerical wave tank (NWT) based on potential flow of incompressible liquid is developed to study nonlinear wave-body interactions in two dimensions. The NWT uses an efficient field method with high accuracy to solve the Laplace equation together with the concepts of immersed boundary method (IBM) and overlapping grids.

1 THE NUMERICAL METHOD

The harmonic polynomial cell (HPC) method is adopted to represent the velocity potential in the fluid. This was proposed by Shao & Faltinsen (2012, 2014) as an accurate and efficient numerical method to solve the Laplace equation in two or three dimensions. In 2D, the computational domain is discretized by quadrilateral, overlapping cells with eight nodes $i = 1, \dots, 8$ along the edges and one interior node $i = 9$. The velocity potential inside each cell is represented as a sum of harmonic polynomials with undetermined coefficients, i.e.

$$\varphi(x,z) = \sum_{i=1}^{8} \sum_{j=1}^{8} c_{j,i} f_j(x,z)\, \varphi_i. \tag{1}$$

The fluid velocity inside a cell is obtained through spatial differentiation of Eq. (1). All harmonic polynomials up to third order and one fourth-order are included, resulting in a spatial accuracy of φ between third and fourth order. f_j is either the real or imaginary part of the j^{th} order harmonic polynomial and $c_{j,i}$ is an entry of the inverse of the matrix $[D]$ with elements $d_{i,j} = f_j(x_i, z_i)$. (x,z) are the local coordinates in the cell's coordinate system with origin located in the interior node. At the cell origin, the only non-zero contribution to Eq. (1) is $f_1 = 1$ which gives the connectivity equation that populates the majority of the global coefficient matrix in the boundary value problem (BVP) for the velocity potential.

In the original HPC papers by Shao & Faltinsen, boundary-fitted grids are used at the body and free surface. In the present work, it is found beneficial to work with structured grids that do not deform in time because the accuracy in the HPC method is optimized when using square or close-to square grids. Furthermore, the grid generation is straightforward, and the coefficients $c_{j,i}$ in Eq. (1) can be precomputed once at the start of the simulation. The latter saves CPU time. An immersed boundary method (IBM) is used to account for surfaces with various geometries in the non-deforming grid. Moreover, to allow non-stretched and non-distorted refined grids near a body and to better handle boundary conditions on moving bodies (including a wavemaker), an overlapping-grid approach is developed. The scenario is illustrated in Fig. 1 for a rounded square. To the left is shown a structured background grid with the outline of an overlapping body-fixed grid that follows the motion of the body indicated. The body-fixed coordinate system $O(x^*, z^*)$ is initially parallel to the Earth-fixed coordinate system $O(x,z)$. To the right the same scenario is viewed from the body-fixed reference frame, where also the distribution of free-surface markers (+) is indicated. In both grids, the free surface is treated as an immersed boundary where the Dirichlet condition for the velocity potential at any time step is imposed directly by applying Eq. (1) in cells with nodes marked with □ along the upper edge. Similarly, the zero-flux body-boundary Neumann condition is imposed by applying the normal derivative of Eq. (1) directly in the grey-shaded ghost cells in the body-fixed reference frame. The nodes marked with black diamonds ⧫ are ghost nodes associated with these ghost cells. The transparent diamonds ◊ indicate nodes where the velocity potential is communicated between the two grids. The potential in

the background grid is interpolated from the body-fixed grid by direct application of Eq. (1) and vice versa. The remaining nodes, indicated by open circles ○, are inactive and removed from the global BVP.

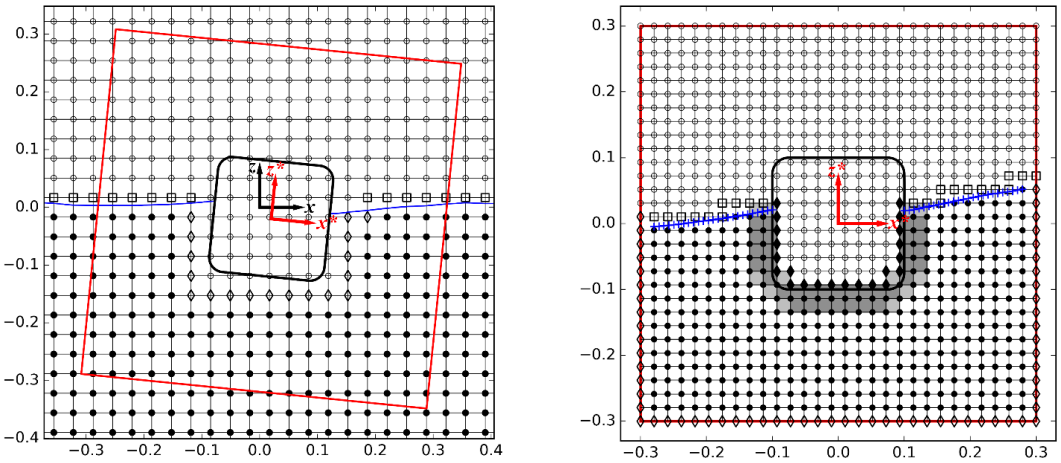

Fig. 1 Left: Background grid seen from the Earth-fixed reference frame. Right: Corresponding body-fixed grid (whose boundary is in red in the left panel) seen from the body-fixed reference frame.

In the Earth-fixed background grid, semi-Lagrangian markers, restricted to move in vertical direction, are used to track the free surface and to enforce its kinematic boundary condition. In the body-fixed grid, the markers at the free surface-body intersections (FSBIs) are fully Lagrangian to allow for a non-wall sided body geometry. The velocity component in x^*-direction of the other markers is enforced to decrease linearly towards zero going far away, so that at a distance away from FSBIs the markers are restricted to move purely in z^*-direction. The body-fixed reference frame is in general non-inertial and the time derivative of the velocity potential in Bernoulli's equation must be rewritten as (Faltinsen & Timokha, 2009):

$$\partial/\partial t|_{non-inertial} = \partial/\partial t|_{inertial} + \vec{u}_r^* \cdot \nabla^*. \tag{2}$$

Here $\vec{u}_r^* = (u_r^*, w_r^*)$ is the velocity relative to the Earth-fixed reference frame of the point in the body-fixed grid where the time derivative is taken. The symbol * indicates that the quantity is resolved along the axes of the $O(x^*, z^*)$ system. Through the markers, also the dynamic free-surface boundary condition for the continuity of the pressure is enforced. The free surface and its potential are evolved forward in time by a standard fourth-order Runge-Kutta scheme.

The hydrodynamic loads induced on a structure by the wave-body interactions are obtained by integrating the total fluid pressure p on the wetted surface. p comes from Bernoulli's equation where the acceleration potential $\varphi_t = \partial\varphi/\partial t$ is found by solving a separate BVP that shares the same coefficient matrix as the BVP for φ. In this BVP, a convective term due to Eq. (2) occurs in the right-hand side for the body-boundary condition in the body-fixed reference frame as well as in the coupling between the background and body-fixed grids with gradients of the potential computed from the spatial derivative of Eq. (1).

In the following, an application involving important nonlinear features and a non-wall sided moving body is discussed. The details of the method and other test cases, including steep-wave generation and incident wave-body interaction, will be presented at the Workshop. These features are relevant to assess the solver applicability for the final aim of the present research, which is for the analysis of moored structures in severe weather conditions.

2 EXAMPLE OF APPLICATION: HEAVING OF A SEMI-SUBMERGED CYLINDER

Sun (2007) used a boundary element method (BEM) to study forced harmonic heave oscillations of a cylinder with radius $R = 0.1m$ in still water at non-dimensional heave amplitude $\epsilon = z_A/R = 0.2$. The same cases are simulated with the present method using the parameters in Table 1, which correspond to converged numerical results.

Table 1 Numerical cases for heaving cylinder in still water.

$\omega^2 R/g$	$\lambda'\ (m)$	$l\ (m)$	$h\ (m)$	$l_x^{bf}\ (m)$	$l_z^{bf}\ (m)$	$\Delta x^{bg}(m)$	$\Delta x^{bf}\ (m)$	Δt	$T/\Delta t$
0.20	3.15	31.47	1.50	2.00	2.00	0.176	0.017	0.0258	55
0.40	1.56	15.62	1.50	1.00	1.00	0.087	0.014	0.0143	70
0.60	1.05	10.53	1.50	0.85	0.85	0.059	0.013	0.0097	85
0.80	0.79	7.90	1.50	0.70	0.70	0.044	0.012	0.0084	85
1.01	0.62	6.19	1.50	0.60	0.60	0.035	0.012	0.0042	150
1.19	0.53	5.29	1.50	0.50	0.50	0.030	0.012	0.0039	150
1.38	0.46	4.56	1.50	0.50	0.50	0.025	0.011	0.0027	200
1.61	0.39	3.90	1.50	0.50	0.50	0.022	0.011	0.0025	200

Here $\omega^2 R/g$ is the non-dimensional square of the heave frequency with g the acceleration of gravity, l and h are the length of the numerical domain and the water depth, l_x^{bf} and l_z^{bf} are the dimensions of the body-fixed grid, $\Delta x^{bg} = \Delta z^{bg}$ is the uniform node spacing in the background grid, $\Delta x^{bf} = \Delta z^{bf}$ is the uniform grid spacing in the body-fixed grid and Δt is the time step. $T = 2\pi/\omega$ is the oscillation period and λ' is the wavelength estimated from the linear deep-water dispersion relation. The tank length is set equal to $10\lambda'$ with the cylinder in the center and the water depth is taken as $15R$. A numerical damping zone with length $2\lambda'$ is used at the domain edges. From Table 1, the background grid is significantly coarser than the body-fixed grid with ratio $\Delta x^{bg}/\Delta x^{bf}$ ranging from 10 for the lowest frequency to 2 for the highest frequency. This is an advantageous feature of using overlapping grids.

A Fourier analysis is performed on the time history of the pressure force to determine the heave added mass A_{33}, heave potential damping B_{33}, second-order harmonic heave force amplitude $F_{z,a2}$ and mean second-order heave force $F_{z,2}^{(0)}$. They are presented in Fig. 2 in non-dimensional form where the mass density of the liquid is ρ and $S_0 = 0.5\pi R^2$ is the mean submerged area of the cylinder. 'Sun (2007)' are Sun's nonlinear BEM results while 'HPC' indicates the solution from the present method. 'lin' are results from a linear theory and 'exp' are experimental results, both by Tasai & Koterayama (1976).

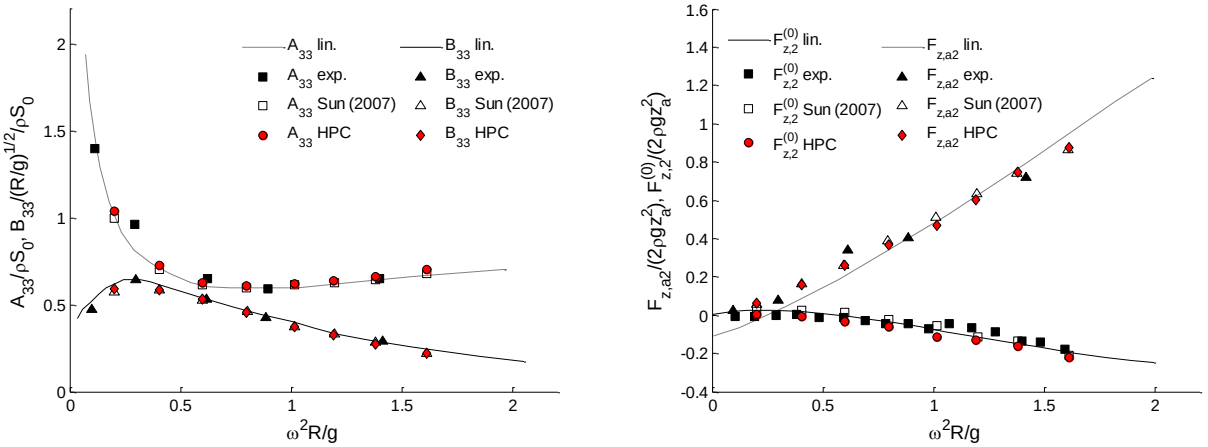

Fig. 2 Heave added mass and damping coefficients (left) and second-order heave force coefficients (right) for semi-submerged heaving cylinder.

The uncertainty bound of the experimental results is unknown. Nevertheless, the agreement is globally good with some minor differences in $F_{z,2}^{(0)}$. These can possibly be due to small differences in the flow near the FSBIs, or due to details of the Fourier analysis. The high-frequency cases in Table 1 require small time steps because large surface curvatures develop near the FSBIs. In order to make the simulations stable, a jet-cutting scheme is introduced when the angle between the free surface and cylinder surface estimated from the wave slope and body curvature becomes less than 5.0 degrees. With this criterion, the simulations are stable. Fig. 3 shows that the

surface elevation with the present method remains in close agreement with the nonlinear BEM results of Sun (2007) until the end of the examined simulation ($\omega^2 R/g = 1.61$).

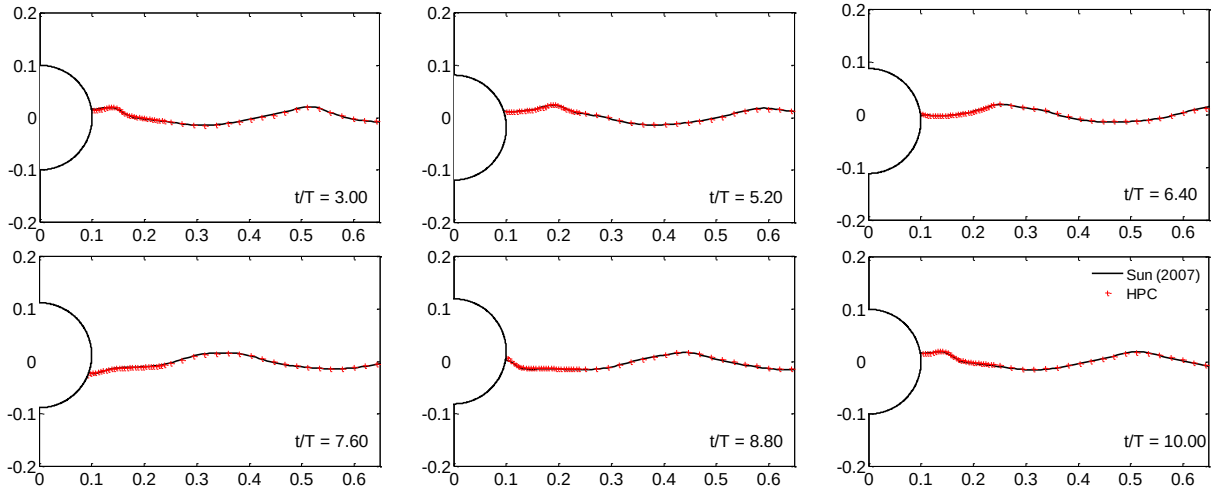

Fig. 3 Surface elevation from present method (+) and from nonlinear BEM by Sun (2007) (-). Here t is time.

3 CONCLUSIONS

The continuous representation of the velocity and acceleration potentials and fluid velocities in the HPC method leads to a straightforward implementation of boundary conditions and evaluation of fluid pressures on wetted surfaces in an IBM. It also facilitates coupling between overlapping grids. Shao & Faltinsen (2012) demonstrated that the HPC method can perform significantly faster than many other alternative methods, and the coupling between grids in the present method does not seem to affect the CPU speed significantly. A heaving cylinder is used as a case study to demonstrate how a dense body-fixed grid can be used to refine the flow features close to a body, with a coarser background grid in the majority of the domain. This represents a general framework to make efficient simulations without loss of accuracy, and is also relevant in 3D or for other applications involving the Laplace equation such as the homogenous solution of the Poisson equation in an incompressible-flow Navier Stokes solver. In the latter case, the overlapping-grid approach will also be applicable in a domain decomposition strategy.

ACKNOWLEDGEMENTS

This work has been carried out at the Centre for Autonomous Marine Operations and Systems (AMOS). The Research Council of Norway is acknowledged as the main sponsor of AMOS. This work was partly supported by the Research Council of Norway through the Centre of Excellence funding scheme, Project number 223254-AMOS.

REFERENCES

Faltinsen, O. M. & Timokha, A. N., 2009. Sloshing (Cambridge University Press).

Shao, Y. L. & Faltinsen, O. M., 2012. Towards efficient fully-nonlinear potential-flow solvers in marine hydrodynamics. In ASME 2012 31st International Conference on Ocean, Offshore and Arctic Engineering (pp. 369-380). American Society of Mechanical Engineers.

Shao, Y. L. & Faltinsen, O. M., 2014. A harmonic polynomial cell (HPC) method for 3D Laplace equation with application in marine hydrodynamics. Journal of Computational Physics, 274, 312-332.

Sun, H., 2007. A boundary element method applied to strongly nonlinear wave-body interaction problems. PhD thesis, Norwegian University of Science and Technology.

Tasai, F. & Koterayama, W., 1976. Nonlinear hydrodynamic forces acting on cylinders heaving on the surface of a fluid. Research Institute for Applied Mechanics. Kyushu University, Fukuaka, Japan.